Synthesis of defect perovskites $(He_{2-x}\square_x)(CaZr)F_6$ by inserting helium into the negative thermal expansion material $CaZrF_6$

Brett R. Hester,[†] Antonio M. Dos Santos, [‡] Jamie J. Molaison,[‡] Justin C. Hancock,[†&] and Angus P. Wilkinson*[,†,§]

[†] School of Chemistry and Biochemistry, Georgia Institute of Technology, Atlanta, GA 30332-0400, United States

[‡]Neutron Science Directorate, Oak Ridge National Laboratory, Oak Ridge, TN 37831, United States

[§]School of Materials Science and Engineering, Georgia Institute of Technology, Atlanta, GA 30332-0245, United States

ABSTRACT: Defect perovskites $(He_{2-x}\square_x)(CaZr)F_6$ can be prepared by inserting helium into $CaZrF_6$ at high pressure. They can be recovered to ambient pressure at low temperature. There are no prior examples of perovskites with noble gases on the A-sites. The insertion of helium gas into $CaZrF_6$ both elastically stiffens the material and reduces the magnitude of its negative thermal expansion. It also suppresses the onset of structural disorder, which is seen on compression in other media. Measurements of the gas released on warming to room temperature and Rietveld analyses of neutron diffraction data at low temperature indicate that exposure to helium gas at 500 MPa leads to a stoichiometry close to $(He_1\square_1)(CaZr)F_6$. Helium has a much higher solubility in $CaZrF_6$ than silica glass or crystobalite. An analogue with composition $(H_2)_2(CaZr)F_6$ would have a volumetric hydrogen storage capacity greater than current US DOE targets. We anticipate that other hybrid perovskites with small neutral molecules on the A-site can also be prepared and that they will display a rich structural chemistry.

Materials with a perovskite derived crystal structure are of great technological and mineralogical significance. This is in part because the parent cubic perovskite structure, with formula ABX_3, can accommodate a very wide range of substitutions and structural distortions. Common distortions include cooperative tilting of the corner sharing BX_6 octahedra[1-3] and offcenter displacement of B and/or A-site cations.[4] Compositions where X is oxide, nitride and halide, or mixtures of them are common place. Metals from almost any region of the periodic table can be found on the B-sites for compositions with appropriately chosen species on the A and X site. Even perovskites with the noble gas Xe on the B-site have been reported.[5] The A-site is also amenable to many substitutions including the incorporation of small organic cations, which is attracting much attention due to their utility in preparing halide-based perovskites with good photovoltaic properties,[6] and also, intriguingly, diatomic nitrogen.[7-9] The inclusion of small neutral species, such as dinitrogen, onto the A-site of defect perovskites has been suggested as a means of controlling the band gap in semiconductors such as WO_3.[7] However, the reported syntheses for dinitrogen containing defect perovskites rely upon the adventitious trapping of dinitrogen on the A-site as a nitrogen rich precursor is thermally decomposed. In this paper we report the direct and well-controlled synthesis of defect perovskites $(He_{2-x}\square_x)(CaZr)F_6$ by inserting helium gas into the initially vacant A-sites of the negative thermal expansion (NTE) material $CaZrF_6$.[10] These materials can be recovered to ambient pressure at low temperature. There have been no prior experimental reports of perovskites containing significant amounts of helium, although there have been computational studies of noble gases included in WO_3.[11]

Metal fluorides with cubic ReO_3-type structures, such as ScF_3,[12] $CaZrF_6$[10] and other $BB'F_6$[13,14] are attracting attention due to their unusual thermal expansion characteristics. As NTE framework materials typically display rich behavior at modest pressures, and potential applications can expose them to significant stress from thermal expansion mismatch, it is important to understand their response to pressure. ReO_3-type materials such as ScF_3 and $CaZrF_6$ are not typically viewed as porous, as the crystallographically determined F-F distances defining the "aperture" between the empty A-sites in this structure are only 4.01 and 4.23 Å respectively at room temperature. However, high pressure neutron diffraction studies of $CaZrF_6$ using gas media reveal very different behavior on compression in nitrogen and helium (Fig. 1a), indicating that the material is porous to helium at room temperature. In nitrogen, at 300 K the unit cell volume decreases linearly on compression and the bulk modulus estimated from these data (K_0 = 36.7(2) GPa) is similar to that previously reported for compression in silicone oil using a Diamond Anvil Cell (K_0 = 36.5(5) GPa) or large volume cell equipped with a BRIM[15] (K_0 = 37.6(6) GPa).[10] In line with the disordering seen at > 400 MPa in silicone oil at room temperature, compression in nitrogen at 160 K led to amorphization at ~500 MPa (see Fig. S1).

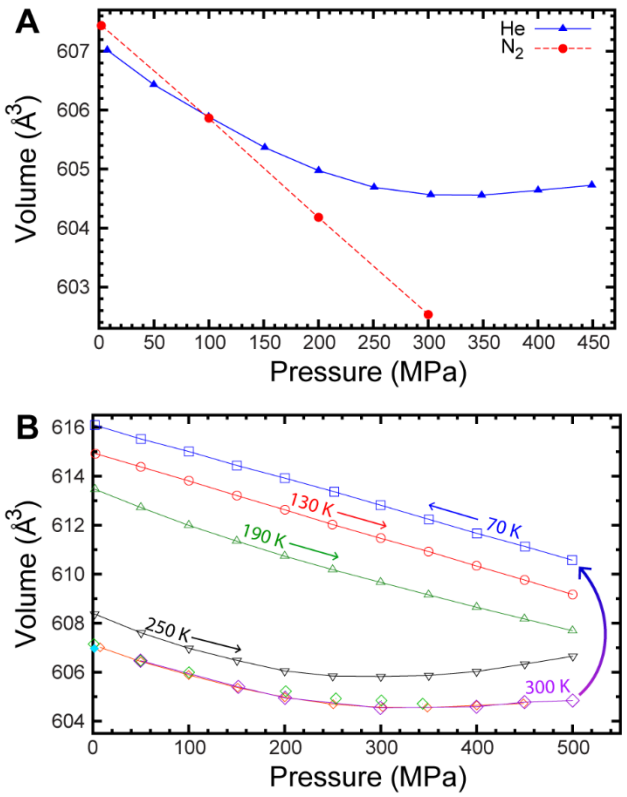

Figure 1. A) Unit cell volume of $CaZrF_6$ with increasing pressure in helium at 300 K (blue) and nitrogen at 290 K (red) gas. B) Change in unit cell volume for $CaZrF_6$ in helium at 300 K on compression (orange), decompression (green), and recompression (purple), cooled at pressure to 70 K, decompressed at 70 K (blue), compressed at 130 K (red), compressed at 190 K (dark green), compressed at 250 K (black), and returned to ambient pressure at 300 K (cyan). Error bars are smaller than the symbols.

In contrast to the behavior in nitrogen, when compressed in helium at 300 K the unit cell volume for $CaZrF_6$ initially decreases, but above ~350 MPa it increases on further compression. This surprising result can be attributed to the insertion of helium into $CaZrF_6$. This behavior is reproducible on decompression and recompression at 300 K (Fig. 1b). It is worth noting that expansion on compression in fluid media, due to the insertion of water, has also been seen in zeolites[16] and that an ammonium metal formate has recently been shown to take up neon at high pressure, but not argon.[17] In silicone oil at 300 K, and nitrogen at low temperature (Fig. S1), compression to ~500 MPa leads to a loss of order in the crystal structure,[10] which does not reverse on decompression. However, the insertion of helium stabilizes the structure against this process; a comparison of diffraction data at 0.075 MPa (Fig. S2) and 500 MPa (Fig. S3) at 300 K in helium reveal no loss of crystallinity, and the sample did not lose crystallinity, as judged by the absence of any significant change in peak to background ratio, throughout the reported neutron diffraction measurements in helium (Fig. S4). The stabilization of porous silicates against disordering, or amorphization, on compression by the insertion of guest species has previously been reported for a number of materials, for example, silicalite.[18]

After cooling from 300 to 70 K under a pressure of ~475 MPa, the decrease of the unit cell volume on decompression is linear and implies a bulk modulus of 55.5(2) GPa, which is much higher than that observed at 300 K in nitrogen. This behavior, and that revealed by diffraction measurements as the sample was compressed/decompressed at successively higher temperatures (Fig. 1b and Fig. S5) is consistent with the helium being trapped, on the time scale of the experiment (~40 minutes for data collection and a pressure increase of 50 MPa), in the $CaZrF_6$ framework at 130 K and below. The inclusion of helium not only stiffens the material (K_{70K} = 55.5(2) GPa, K_{130K} = 53.0(1) GPa), it modifies the thermal expansion. Prior ambient pressure neutron diffraction measurements indicate that $CaZrF_6$ has an expansion coefficient, α_v, of -52(2) ppm K^{-1} at 100 K. However, the current data show that a sample prepared by inserting helium into $CaZrF_6$ at ~475 MPa and then cooling under pressure, has an expansion coefficient, α_v, of -31(1) ppm K^{-1} at 100 K. The reduction in the magnitude of the expansion is not surprising, as the insertion of any species into the A-site cavities will impeded the transverse vibrational motion of the fluoride that is responsible for the NTE. It is notable that the deliberate insertion of lithium into redox active ReO_3-type fluorides has recently been demonstrated as a strategy for controlling the thermal expansion of such materials.[19]

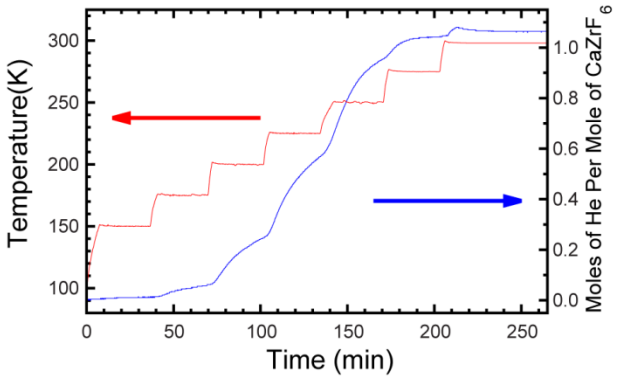

Figure 2. Helium release versus time and temperature for a sample of $(He_{2-x}\square_x)(CaZr)F_6$ that had been cooled down to 100K under a helium pressure of ~500 MPa.

The amount of helium inserted into $CaZrF_6$ was quantified by warming gas-loaded samples to room temperature and monitoring the pressure in the sample head space (see supplementary material). The major source of uncertainty in these measurements is likely to be the determination of the sample head space volume, which could be in error by up to 10%. Fig. 2 shows the amount of helium released as a function of time and temperature for a sample loaded with helium at ~500 MPa. These data indicate that the $CaZrF_6$ had 54(5)% of its A-sites filled, corresponding to a defect perovskite with composition $(He_{1.08}\square_{0.92})(CaZr)F_6$. On the time scale of the measurements, there is no helium release at 150 K and the gas can be considered to be trapped. On warming, the rate of helium release increases quite dramatically, but even at close to room temperature the time scale for helium release is minutes not seconds.

Helium uptake measurements were also performed for loadings at 300 MPa and 150 MPa. As expected, at lower pressures a smaller fraction of the available A-sites were filled (21(2)% and 0.8(1)% respectively). However when the same sample of $CaZrF_6$ was subsequently loaded with helium at 400 MPa, the gas uptake was much lower than anticipated (only 3.9(4)% of A-sites filled). As the data in Fig 2 indicate that the time scale for helium insertion at room

temperature is of the order of minutes, and $CaZrF_6$ is known to disorder on compression to 400-500 MPa when there is nothing on the A-sites, the reduction in uptake during the final loading with helium at 400 MPa is almost certainly due to sample degradation. When the helium pressure is increased rapidly an irreversible disordering occurs before enough helium is inserted to stabilize the ReO_3-type structure. This interpretation suggests that the A-site occupancies shown in Fig. S6 for 500, 300, and 150 MPa represent a lower limit of what should be achievable with a pristine sample.

In order to both locate and confirm the quantity of helium in $(He_{2-x}\square_x)(CaZr)F_6$, Rietveld analyses of the neutron diffraction data were performed. Fig. 3A shows a fit to 70 K, 500 MPa data with an Fm-3m model for $CaZrF_6$ and no helium on the A-sites. The residual plot shows significant features well above the noise level of the data. Fig. 3B shows a fit where helium was placed on the A-site of the perovskite with an occupancy of 0.54 and its isotropic thermal parameter refined (U_{iso} = 0.045(3) Å^2). The inclusion of helium in the model significantly improved the fit quality. Refinements were carried out for all of the neutron diffraction data acquired in helium. The A-site occupancies (Fig. S8) clearly show that at both 250 and 300 K helium goes into the structure as the pressure is increased, but at 70, 130 and 190 K there is little change in occupancy as the pressure varied.

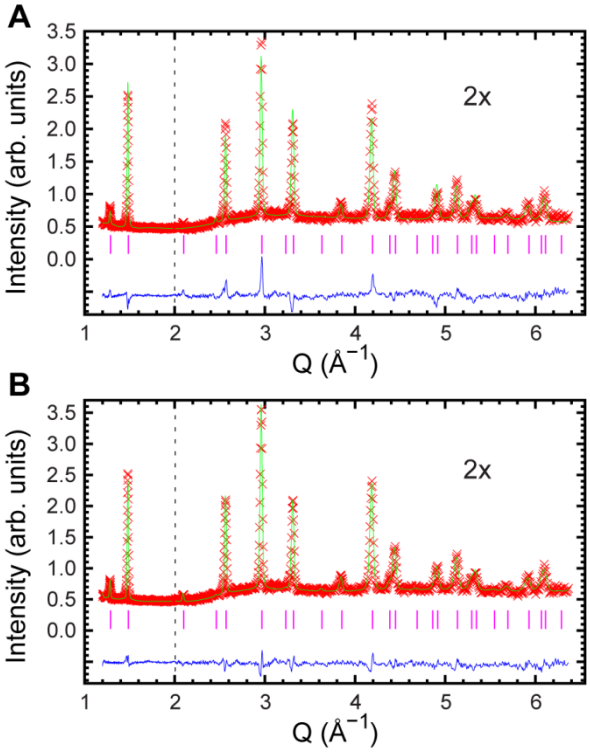

Figure 3. Rietveld fits to powder neutron diffraction data recorded on SNAP using a Fm-3m model for $CaZrF_6$ A) containing no helium, detector bank 2 (2θ ~48°), R_F2= 27.4%, and B) using $(He_{2-x}\square_x)(CaZr)F_6$ with x = 1.08 detector bank 2, R_F2=18.0 %.

The penetration of helium into materials that are not typically viewed as porous is quite well known and can hinder the use of helium as a truly inert hydrostatic medium for high pressure experiments. For example, molecular solids such as C_{60}[20] and arsenolite[21,22] take up significant amounts of helium. The silica clathrate melanophlogite,[23] which has a type-I gas hydrate related structure, and both silica glass[24,25] and cristobalite,[26] which are denser than the clathrate framework, behave differently when compressed in helium versus media containing much larger molecules. In helium, they display higher bulk moduli, due to the insertion of helium, and it has been estimated that for silica glass the lower limit for helium solubility at 10 GPa is 1 mole of helium per mole of SiO_2.[24]The penetration of hydrogen at 250 °C and high pressures into silica glass[27] and cristobalite[28] has also been reported.

Helium is much more soluble in $CaZrF_6$ than silica glass at low (< 1 GPa) pressure, with approximately 1 mole of helium per mole of $CaZrF_6$ being taken up at ~500 MPa. This helium can be retained in the structure by cooling and then subsequently released on warming to room temperature, suggesting applications in gas storage. Temperature regulated uptake and release of gases in zeolitic materials is quiet well known,[29,30] particularly in materials showing a trapdoor like effect involving the thermally activated motion of extra-framework cations, and it has previously been proposed as a method for hydrogen storage.[30] It is notable that if a perovskite with one hydrogen per A-site could be prepared, $(H_2)_2(CaZr)F_6$, it would have a volumetric storage capacity of 0.044 kg H_2/L, which exceeds the US DOE 2025 technical target for hydrogen storage in fuel cell vehicles (0.04 kg H_2/L).[31]

The preparation of $(He_{2-x}\square_x)(CaZr)F_6$ is a significant extension of perovskite chemistry to include the controlled synthesis of materials with small gas molecules on the A-site. Modification of composition, to tune the effective pore size of the ReO_3-type framework, and the temperature at which gases are inserted into the parent material, should allow other gases to be incorporated into perovskites and their uptake and release pressures to be controlled. We anticipate that this new family of hybrid perovskites will display a rich crystal chemistry as composition, temperature and pressure are varied.

ASSOCIATED CONTENT

Supporting Information. $CaZrF_6$ synthesis, neutron diffraction methodology, gas uptake measurements, example Rietveld plots, helium content versus loading pressure, lattice constants with and without helium, helium A-site fractional occupancies as a function of temperature and pressure and crystallographic parameters. This material is available free of charge via the Internet at http://pubs.acs.org.

AUTHOR INFORMATION

Corresponding Author

* angus.wilkinson@chemistry.gatech.edu

Present Addresses

& Department of Chemistry, Northwestern University, 2145 Sheridan Road, Evanston, IL60208

Funding Sources

The work at Georgia Tech was partially supported under NSF DMR-1607316. A portion of this research used resources at the Spallation Neutron Source, a DOE Office of Science User Facility operated by the Oak Ridge National Laboratory.

ACKNOWLEDGMENT

We are grateful for experimental assistance from the sample environment team at the Spallation Neutron Source. We also appreciate the

assistance of Craig Brown and Juscelino Leao during preliminary experiments on BT1 at the NIST NCNR.

REFERENCES

(1) Howard, C. J.; Stokes, H. T. *Acta Crystallogr.* **1998**, *B54*, 782.

(2) Glazer, A. M. *Acta Crystallogr.* **1975**, *A31*, 756.

(3) Glazer, A. M. *Acta Crystallogr.* **1972**, *B28*, 3384.

(4) Howard, C. J.; Stokes, H. T. *Acta Crysatollgr.* **2005**, *A61*, 93.

(5) Britvin, S. N.; Kashtanov, S. A.; Krzhizhanovskaya, M. G.; Gurinov, A. A.; Glumov, O. V.; Strekopytov, S.; Kretser, Y. L.; Zaitsev, A. N.; Chukanov, N. V.; Krivovichev, S. V. *Angew. Chem. Int. Ed.* **2015**, *54*, 14340.

(6) Lee, M. M.; Teuscher, J.; Miyasaka, T.; Murakami, T. N.; Snaith, H. J. *Science* **2012**, *338*, 643.

(7) Mi, Q. X.; Ping, Y.; Li, Y.; Cao, B. F.; Brunschwig, B. S.; Khalifah, P. G.; Galli, G. A.; Gray, H. B.; Lewis, N. S. *J. Am. Chem. Soc.* **2012**, *134*, 18318.

(8) Tessier, F.; Le Gendre, L.; Chevire, F.; Marchand, R.; Navrotsky, A. *Chem. Mater.* **2005**, *17*, 3570.

(9) Le Gendre, L.; Marchand, R.; Piriou, B. *Eur. J. Solid State Inorg. Chem.* **1997**, *34*, 973.

(10) Hancock, J. C.; Chapman, K. W.; Halder, G. J.; Morelock, C. R.; Kaplan, B. S.; Gallington, L. C.; Bongiorno, A.; Han, C.; Zhou, S.; Wilkinson, A. P. *Chem. Mater.* **2015**, *27*, 3912.

(11) Ping, Y.; Li, Y.; Gygi, F.; Galli, G. *Chem. Mater.* **2012**, *24*, 4252.

(12) Greve, B. K.; Martin, K. L.; Lee, P. L.; Chupas, P. J.; Chapman, K. W.; Wilkinson, A. P. *J. Am. Chem. Soc.* **2010**, *132*, 15496.

(13) Hester, B. R.; Hancock, J. C.; Lapidus, S. H.; Wilkinson, A. P. *Chem. Mater.* **2017**, *29*, 823.

(14) Hu, L.; Chen, J.; Xu, J.; Wang, N.; Han, F.; Ren, Y.; Pan, Z.; Rong, Y.; Huang, R.; Deng, J.; Li, L.; Xing, X. *J. Am. Chem. Soc.* **2016**, *138*, 14530.

(15) Wilkinson, A. P.; Morelock, C. R.; Greve, B. K.; Jupe, A. C.; Chapman, K. W.; Chupas, P. J.; Kurtz, C. *J. Appl. Crystallogr.* **2011**, *44*, 1047.

(16) Lee, Y.; Vogt, T.; Hriljac, J. A.; Parise, J. B.; Artioli, G. *J. Am. Chem. Soc.* **2002**, *124*, 5466.

(17) Collings, I. E.; Bykova, E.; Bykov, M.; Petitgirard, S.; Hanfland, M.; Paliwoda, D.; Dubrovinsky, L.; Dubrovinskaia, N. *Chemphyschem* **2016**, *17*, 3369.

(18) Haines, J.; Cambon, O.; Levelut, C.; Santoro, M.; Gorelli, F.; Garbarino, G. *J. Am. Chem. Soc.* **2010**, *132*, 8860.

(19) Chen, J.; Gao, Q.; Sanson, A.; Jiang, X.; Huang, Q.; Carnera, A.; Rodriguez, C. G.; Olivi, L.; Wang, L.; Hu, L.; Lin, K.; Ren, Y.; Lin, Z.; Wang, C.; Gu, L.; Deng, J.; Attfield, J. P.; Xing, X. *Nat. Commun.* **2017**, *8*, 14441.

(20) Schirber, J. E.; Kwei, G. H.; Jorgensen, J. D.; Hitterman, R. L.; Morosin, B. *Phys. Rev. B* **1995**, *51*, 12014.

(21) Sans, J. A.; Manjon, F. J.; Popescu, C.; Cuenca-Gotor, V. P.; Gomis, O.; Munoz, A.; Rodriguez-Hernandez, P.; Contreras-Garcia, J.; Pellicer-Porres, J.; Pereira, A. L. J.; Santamaria-Perez, D.; Segura, A. *Phys. Rev. B* **2016**, *93*, 5.

(22) Gunka, P. A.; Dziubek, K. F.; Gladysiak, A.; Dranka, M.; Piechota, J.; Hanfland, M.; Katrusiak, A.; Zachara, J. *Cryt. Growth Des.* **2015**, *15*, 3740.

(23) Yagi, T.; Iida, E.; Hirai, H.; Miyajima, N.; Kikegawa, T.; Bunno, M. *Phys. Rev. B* **2007**, *75*, 6.

(24) Sato, T.; Funamori, N.; Yagi, T. *Nat. Commun.* **2011**, *2*, 5.

(25) Shen, G.; Mei, Q.; Prakapenka, V. B.; Lazor, P.; Sinogeikin, S.; Meng, Y.; Park, C. *Proc. Natl. Acad. Sci.* **2011**, *108*, 6004.

(26) Sato, T.; Takada, H.; Yagi, T.; Gotou, H.; Okada, T.; Wakabayashi, D.; Funamori, N. *Phys. Chem. Minerals* **2013**, *40*, 3.

(27) Efimchenko, V. S.; Fedotov, V. K.; Kuzovnikov, M. A.; Zhuravlev, A. S.; Bulychev, B. M. *J. Phys. Chem. B* **2013**, *117*, 422.

(28) Efimchenko, V. S.; Fedotov, V. K.; Kuzovnikov, M. A.; Meletov, K. P.; Bulychev, B. M. *J. Phys. Chem. A* **2014**, *118*, 10268.

(29) Breck, D. W. *Zeolite Molecular Sieves*; John Wiley and Sons: New York, 1974.

(30) Li, G.; Shang, J.; Gu, Q.; Awati, R. V.; Jensen, N.; Grant, A.; Zhang, X.; Sholl, D. S.; Liu, J. Z.; Webley, P. A.; May, E. F. *Nat. Commun.* **2017**, *8*, 15777.

(31) *Fuel Cell Technologies Office. Multi-Year Research, Development, and Demonstration Plan. Planned Program Activities for 2011-2020*; US Department of Energy, EERE, 2012.

Authors are required to submit a graphic entry for the Table of Contents (TOC) that, in conjunction with the manuscript title, should give the reader a representative idea of one of the following: A key structure, reaction, equation, concept, or theorem, etc., that is discussed in the manuscript. Consult the journal's Instructions for Authors for TOC graphic specifications.

Insert Table of Contents artwork here